Phase Behavior of Octyldimethyl *para*-Amino Benzoate, Polyoxyethylene-10-stearyl Ether, Olive Oil, and Water

J. Yang[a], H. Yang[a], S.E. Friberg[a,*], and Patricia A. Aikens[b]

[a]Center for Advanced Materials Processing, Clarkson University, Potsdam, New York 13699-5814, and [b]ICI Surfactants, Wilmington, Delaware 19850

ABSTRACT: The phase diagrams of octyl dimethyl *para*-amino benzoate (ODP)/polyoxyethylene-10-stearyl ether (Steareth 10)/olive oil/water, and of ODP/polyoxyethylene-4-lauryl ether (Laureth 4)/water systems were determined. ODP was solubilized in the lamellar liquid crystal of Steareth 10 water and of Laureth 4 water to 15 and 12% by weight, respectively. Low-angle x-ray diffraction was used to determine the location of the ODP molecules in the liquid crystal. ODP penetrated between the hydrocarbon chains of the surfactants, while olive oil was solubilized both at that site and between the terminal methyl group layers. The location of ODP in the liquid crystal was also reflected in ultraviolet absorption in the 260–350 nm region of the spectrum, which was compared to absorption in a polar solvent, polyethylene glycol (260–340 nm), and in a nonpolar solvent, decane (260–328 nm).
JAOCS 74, 809–816 (1997).

KEY WORDS: Cosmetics, detergents, emulsions, liquid crystals, micellar solutions, microemulsions, solubilization, sunscreens, UV absorption.

The first use of sunscreen was reported in 1920 in the United States (1). Rapid development has occurred in the last 10–15 yr because the rise in new cases of skin cancer has in part been attributed to the sun's damaging rays (2). In 1978, only 21 chemicals for sunscreen were listed as "safe and effective at the recommended dosage and intended use"; 19 of these chemicals were ultraviolet (UV) absorbers and two were physical sun blockers. Since then, much attention has been focused on increasing the effectiveness of the 19 UV-absorbing chemicals (2–6).

Protection by a sunscreen compound, however, is not determined by its structure alone. The formulation is also important because the structural changes during evaporation (7) of the volatile part of the sunscreen may have a decisive influence on both performance and consumer acceptance of the product (8). Although not widely realized, the structure of the initial formulation of an emulsion, microemulsion, or liposomal volative does not provide information about the final structure after evaporation nor about the changes in the structure during the evaporative removal of volatile substances (7).

*To whom correspondence should be addressed.
E-mail: FBG@agent.clarkson.edu.

Another factor in the effectiveness of sunscreen products is their interaction with the stratum corneum layer of the skin (2) because the lipid part of the stratum corneum is responsible for the different barriers (9–12) against skin penetration. Changes in the structure of stratum corneum due to penetration may have side effects (13) because the barrier is based on the lamellar structure of the stratum corneum.

With these facts in mind, we found it useful to study the relation between a simple sunscreen molecule, olive oil, water, and common nonionic surfactants, polyoxyethylene alkyl ethers. Olive oil was chosen because it is widely used in cosmetics (14–18), pharmaceuticals (19,20), and foods (21,22). Octyl dimethyl *para*-amino benzoate (ODP) is a widely used sunscreen because it is waterproof and, hence, has superior performance under humid conditions.

The complex structure of ODP (Scheme 1), with its weak polar components, gives no indication of its location in a lamellar structure such as the lipid part of the stratum corneum. The present investigation provides information on this aspect, and in addition, the evaporation evaluations reveal the highest amount of sunscreen in the original formulation to leave a final continuous film on the skin in the Laureth 4/ODP/water system.

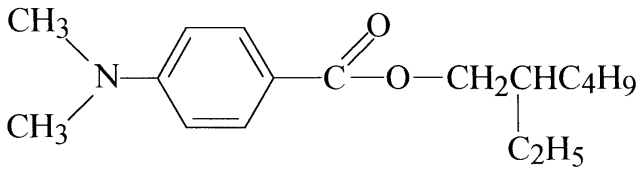

SCHEME 1

EXPERIMENTAL PROCEDURES

Materials. The nonionic surfactants, polyoxyethylene-10-stearyl ether (Steareth 10), Brij 76®, and polyoxyethylene-4-lauryl ether (Laureth 4), Brij 30®, were from ICI Surfactants (Wilmington, DE). The sunscreen ODP was from ISP van Dyk, Inc. (Belleville, NJ). Olive oil was from Sigma (St. Louis, MO). These chemicals were used without further purification. Water was doubly distilled.

Phase diagram determination. The water/oil (W/O) microemulsion region (L_2) of the phase diagrams was determined

by titration of mixtures of ODP and nonionic surfactant or olive oil with water. The extent of the liquid crystal phase was found by optical microscopy of a sample between crossed polarizers by observation of birefringence. The borderline to the three-phase region, following the solutions of ODP and water (L_2/H_2O) two-phase area and the three-phase area with liquid crystals, was also determined by observation of birefringence. The other two borderlines were determined by low-angle x-ray diffraction by using knickpoints in the curves of interlayer spacing of the liquid crystal vs. composition, as were the phase boundaries of the liquid crystal phase.

All phase diagrams were determined at room temperature (22 ± 1°C).

Low-angle x-ray diffraction. A small amount of the sample mixture was drawn into a fine glass capillary tube (0.7-mm diameter). Low-angle x-ray diffraction data were obtained from a Kiessig low-angle camera from Richard Seifert, Ahrensburg, Germany. Ni-filtered Cu radiation ($\lambda = 1.542$ Å) was used, and the reflections were determined by a Tennelec position-sensitive detector system (model psd-100) with gas ionization.

UV absorption studies. UV spectra were recorded on a Milton Roy Spectronic 3000 Array (Rochester, NY). Liquid samples were measured in a 10×1 mm quartz cell. The liquid crystal samples were measured between two quartz slides of varied thickness as measured by a micrometer; samples without sunscreen were used as reference. The concentration of sample was controlled so that the absorbance was below 1.0.

RESULTS

Phase diagrams of Steareth 10/olive oil/ODP/water systems. The phase diagram of ODP/Steareth 10/water is shown in Figure 1. The solubility of ODP and water in Steareth 10 was 10 and 44%, respectively. Steareth 10 was soluble to 23% in ODP

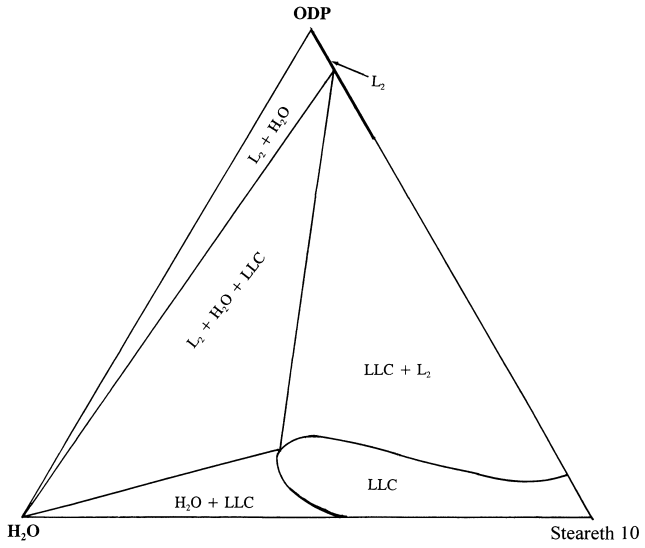

FIG. 1. Phase diagram of Steareth 10/ODP/water system. L_2, solubility area of Steareth in ODP. LLC, lamellar liquid crystal region. ODP, octyl dimethyl *para*-aminobenzoate. Steareth 10; polyoky-ethylene-10-stearyl ether.

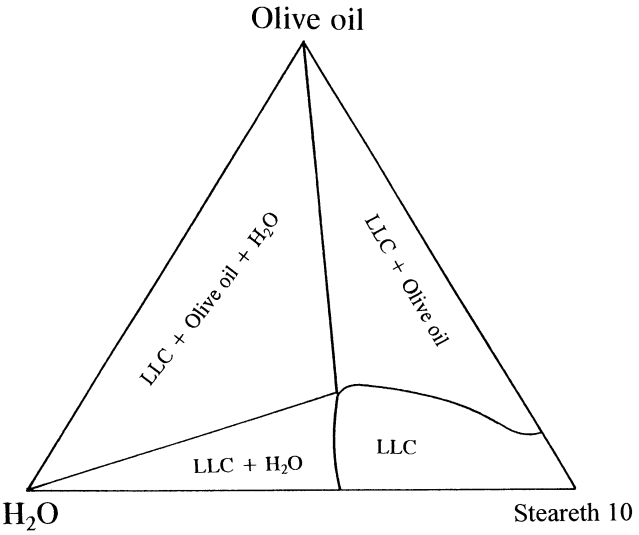

FIG. 2. Phase diagram of Steareth 10/olive oil/water system. See Figure 1 for abbreviations.

to form a solution region, L_2, in the upper right corner of the phase diagram. H_2O was solubilized into this region only to a small extent (<1%). Both ODP and Steareth 10 were essentially insoluble in water. With these phases present, one finds a two-phase ($L_2 + H_2O$) region on the left side of the phase diagram followed by a large three-phase region (LLC + L_2 + H_2O). The large area of the surfactant/water lamellar liquid crystal (LLC) region solubilized up to 15% ODP, and an LLC + H_2O two-phase region was, hence, found along the water/surfactant axis. Finally, the L_2 and the LLC regions formed a two-phase (L_2 + LLC) area. Note that the three-phase ($L_2 + H_2O$ + LLC) corner is not located at maximum Steareth 10 in the ODP.

Figure 2 shows the phase behavior of the Steareth 10/olive oil/H_2O system. Steareth 10 is insoluble in both H_2O and olive oil. The solubility of olive oil in Steareth 10 is 12%. Therefore, the phase diagram showed only one extended one-

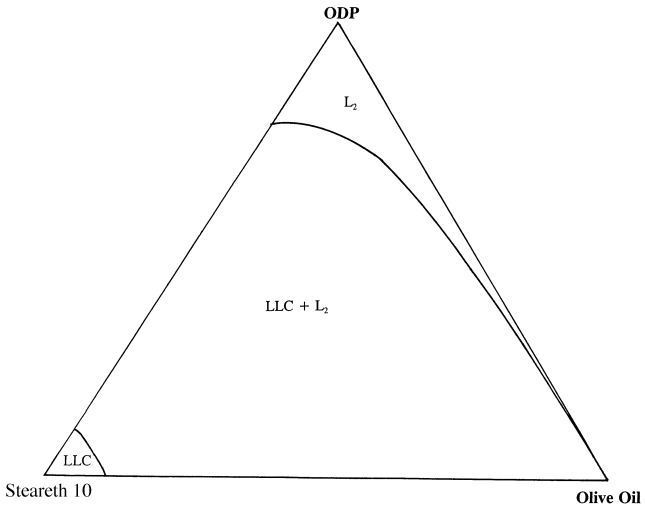

FIG. 3. Phase diagram of Steareth 10/olive oil/ODP system. See Figure 1 for abbreviations.

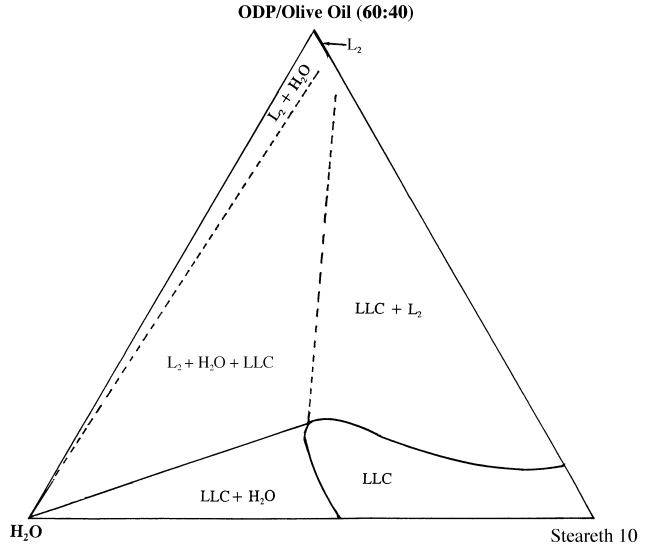

FIG. 4. Partial phase diagram of Steareth 10/olive oil/ODP/water system. Weight ratio of ODP/olive oil 60:40. The three-phase area is out of the plane. See Figure 1 for abbreviations.

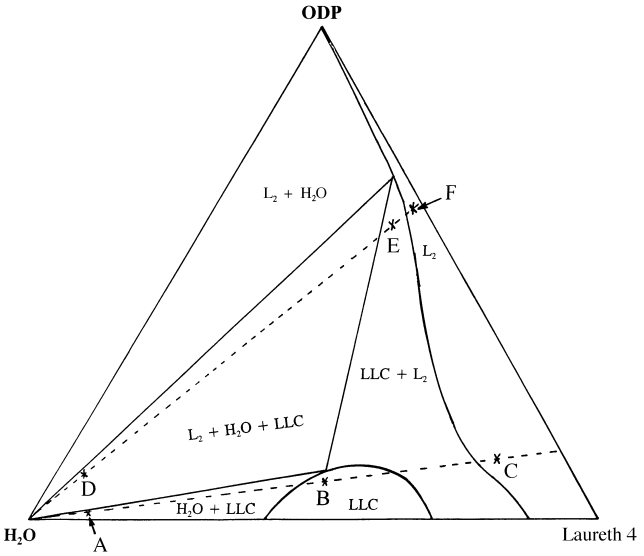

FIG. 6. Phase diagram of Laureth 4/ODP/water system. L_2, W/O microemulsion region. Laureth 4, polyoxyethylene-4-lauryl ether. For other abbreviations see Figure 1.

phase region (LLC), two two-phase regions [(H_2O + LLC) and (olive oil + LLC)], and one three-phase region (LLC + H_2O + olive oil).

The phase behavior of olive oil/Steareth 10/ODP is simple, as seen in Figure 3. ODP and olive oil are mutually soluble, and an isotropic liquid solution region L_2 was found, with the solubility of Steareth 10 in ODP being rapidly reduced with increased amounts of olive oil. At the Steareth 10 corner, there is an LLC region. Because of these conditions, a large (LLC + L_2) two-phase region was found.

Figure 4 shows the phase behavior of the H_2O/(ODP + olive oil)/Steareth 10 system with a 60:40 weight ratio of ODP to olive oil. The phase diagram, as expected, shows features between those of the Steareth 10/ODP/H_2O system (Fig. 1) and the Steareth 10/olive oil/H_2O system (Fig. 2). The three-phase area is only indicated because it is not in the plane of this pseudo-ternary phase diagram.

Figure 5 shows the complete phase diagram of the Steareth 10/ODP/olive oil/H_2O system in a three-dimensional presentation. The liquid crystal phase is found at the right side of the bottom part, and the isotropic liquid region (L_2) lies in the plane of ODP/olive oil/Steareth 10. The L_2 region is continuously reduced with increasing olive oil content. The three-phase region (L_2 + LLC + H_2O) is in the middle part and extends from the Steareth 10/ODP/H_2O plane to the Steareth 10/olive oil/H_2O plane.

The phase diagram of Laureth 4/ODP/H_2O is shown in Figure 6. ODP and Laureth 4 were completely soluble in each other, and

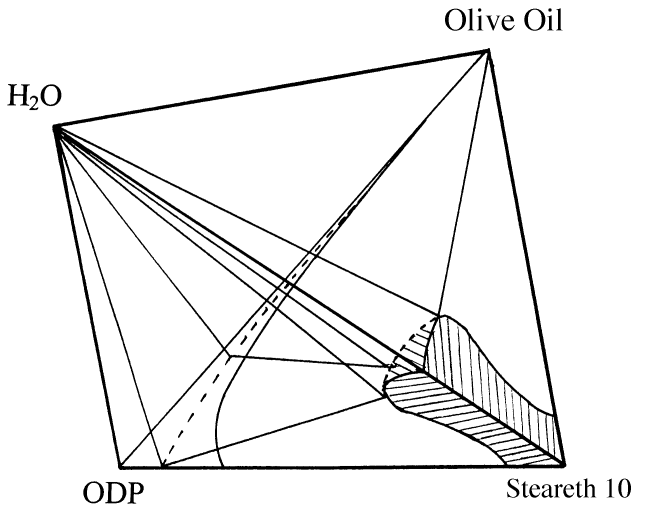

FIG. 5. Three-dimensional phase diagram of system Steareth 10/olive oil/ODP/water. Shadowed area is LLC. See Figure 1 for abbreviations.

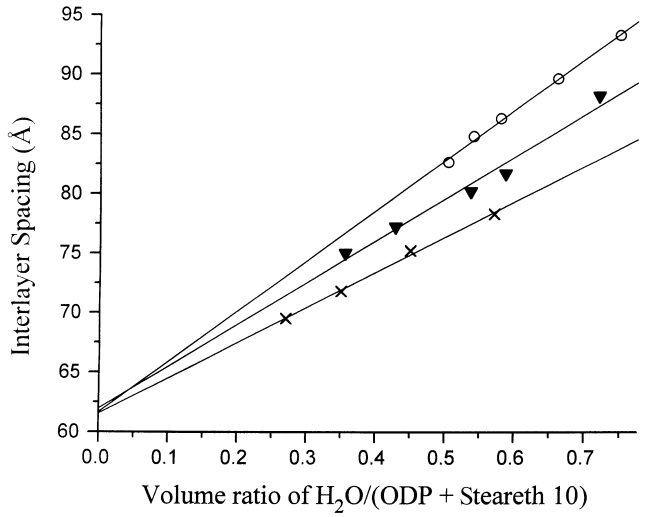

FIG. 7. Interlayer spacing vs. volume ratio of water/(ODP + Steareth 10); ODP/Steareth 10:0 0:100, X; 10:90, ▼; 20:80, ○. For abbreviations see Figure 1.

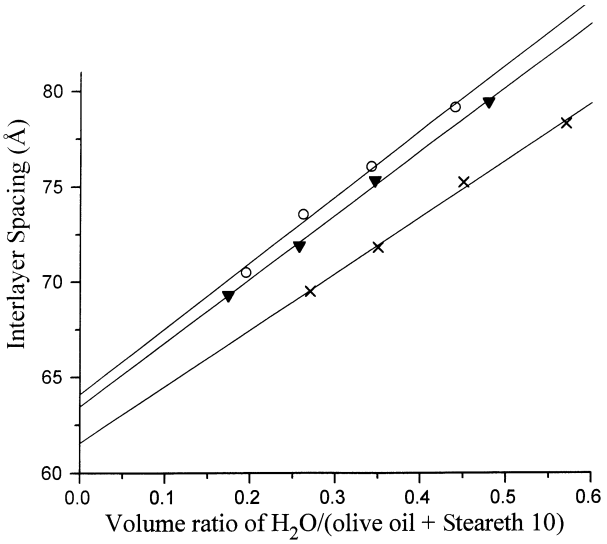

FIG. 8. Interlayer spacing vs. volume ratio of water/(olive oil + Steareth 10); olive oil/Steareth 10: X, 0:100; ▼, 10:90; ○, 20:80. For abbreviation see Figure 1.

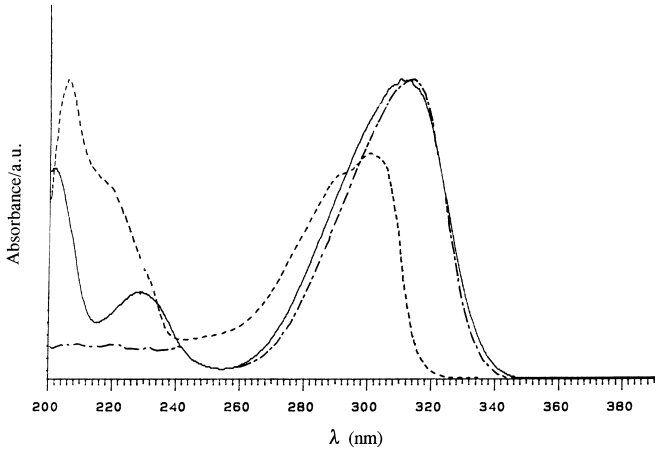

FIG. 10. Ultraviolet (UV) spectra of ODP in the water/Steareth 10 lamellar liquid crystal; LLC, ————; decane, – – – – –; polyethylene glycol methyl ether, —— – ——. See Figure 1 for abbreviations.

water was solubilized in this L_2 region to a maximum of 17% by weight, and in pure Laureth 4 to 13%. An LLC region extends from 30 to 58% water along the water-surfactant axis, and solubilizes a maximum of 12% by weight of ODP. ODP and Laureth 4 are essentially insoluble in H_2O. On the left side of the phase diagram, there is a two-phase ($L_2 + H_2O$) region, and a large three-phase region (LLC + L_2 + H_2O) in which a constant interlayer spacing was found due to the contact with only one point of the liquid crystal region. In addition, there are two two-phase regions [(LLC + L_2) and (LLC + H_2O)] in equilibrium with LLC.

The interlayer spacings from the LLC of Steareth 10 with water and ODP given in Figure 7. An increased ratio of ODP/Steareth 10 led to an increasing slope of the plot but gave identical interlayer spacing extrapolated to zero water content. The liquid crystal with olive oil, on the other hand, showed increased interlayer spacing but constant slope as the amount of olive oil was increased (Fig. 8).

The interlayer spacings from the Laureth 4 LLC with water and ODP are given in Figure 9. Increasing the ratio of ODP/Laureth 4 led to an increasing slope but gave an identical interlayer spacing when extrapolated to zero water content, which is a similar result to that of the Steareth 10/ODP/water system.

Figure 10 shows UV spectra of ODP in the LLC of Steareth 10. The UV region can be divided into three parts: UV A (320–400 nm), UV B (290–320 nm), and UV C (200–290 nm). In polyethylene glycol methyl ether, absorption is in the UV B and part of the UV A/C region from 342 to 260 nm. In decane, one absorption is in the UV C range, and another absorption is in the UV B and part of the UV A/C range (322–260 nm). In LLC of Steareth 10, the spectrum of ODP has one absorption in UV C and another one in UV B and part of the UV A/C range (342–260 nm). ODP has the same order of molar absorbance coefficient, $\varepsilon = 2.56 \sim 3.44 \times 10^4$ $dm^3mol^{-1}cm^{-1}$, in

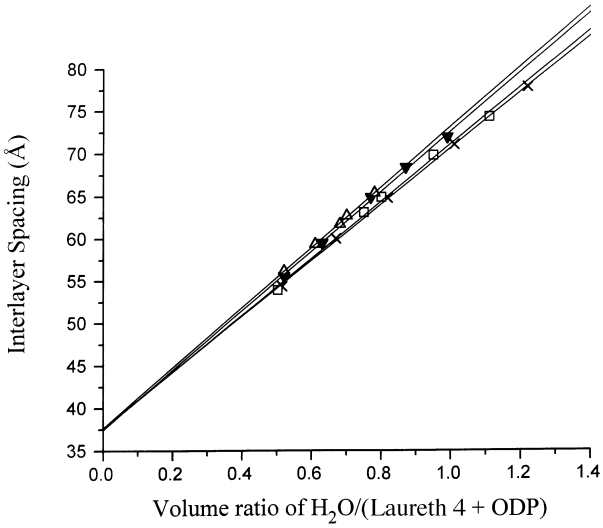

FIG. 9. Interlayer spacing vs. volume ratio of water/(ODP + Laureth 4); olive oil/Laureth 4: X, 0:100; □, 5:95; ▼, 10:90; △, 15:85. For abbreviations see Figures 1 and 6.

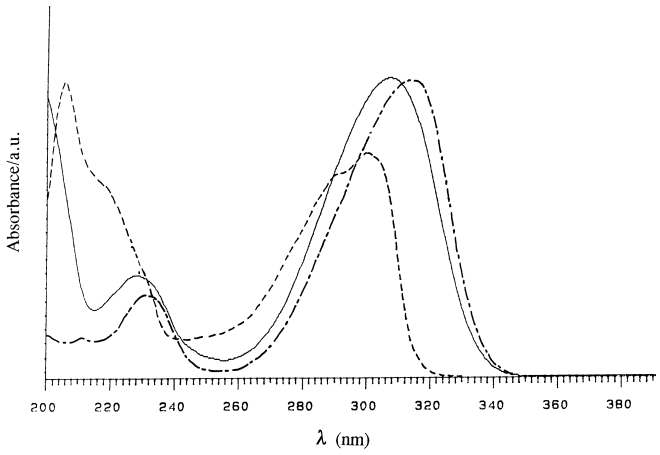

FIG. 11. UV spectra of ODP in the water/Laureth 4 lamellar liquid crystal. Vehicle: LLC, ————; decane, – – – – –; tetraethylene glycol, —— – ——. For abbreviations see Figures 1, 6, and 10.

TABLE 1
The Maximal Absorbance and Molar Absorbance Coefficient of ODP in Different Media

Medium for solubilized ODP[a]	λ_{max} (nm)	ε ($dm^3\ mol^{-1}cm^{-1}$)
LLC in Steareth 10/H_2O (65:25, w/w)	309	3.44×10^4
Decane	300	2.77×10^4
Polyethylene glycol methyl ether (MW = 340)	313	2.56×10^4

[a]The concentration of octyl dimethyl *para*-amino benzoate (ODP) was 0.1% (wt) in lamellar liquid crystal (LLC) and 0.02% (wt) in solution according to different cell thickness to keep the absorbance below 1.0; MW, molecular weight. Steareth 10: polyoxyethylene-10-stearyl ether.

LLC, polyethylene glycol methyl ether, and decane (Table 1). Figure 11 shows UV spectra of ODP in the LLC of Laureth 4. The spectrum is similar to that in the Steareth 10 LLC, with the absorption maximum at a slightly shorter wavelength. ODP has the same order of molar absorbance coefficient, $\varepsilon \cong 3\text{–}4 \times 10^4$ dm^3mol^{-1} in LLC and L_2 (Table 2).

DISCUSSION

The results show a number of features which deserve an analysis. At first, the small difference in the extent of intermolecular interaction between olive oil and ODP caused major changes in the phase diagrams and in the location of the molecules in the liquid crystal. ODP dissolves a certain amount of Steareth 10; however, only a small amount of water can be solubilized in this region. The polarity of ODP is obviously too low to dissolve water, even with the assistance of the surfactant. Olive oil, obviously being even less polar than ODP, does not dissolve Steareth 10. Even the smallest amount of Steareth 10 led to the separation of a liquid crystalline phase. A solution of ODP and olive oil dissolved Steareth 10 to the expected amounts, considering the solubility in the individual compounds.

The difference in polarity between ODP and olive oil was also illustrated by their respective location in the LLC as shown by the interpretation of interlayer spacing values from the low-angle x-ray diffraction data. The x-ray results give the interlayer spacing d (Fig. 12), and these values may be used to obtain information about the degree of water penetration from A into the amphiphilic layer B and of the location of olive oil and ODP molecules. Assuming no change in tilt of the molecules and accepting that changes in the degree of order have only a minor influence on interlayer spacing, one finds:

$$d = d_0(1 + R)/(1 + \alpha R) \quad [1]$$

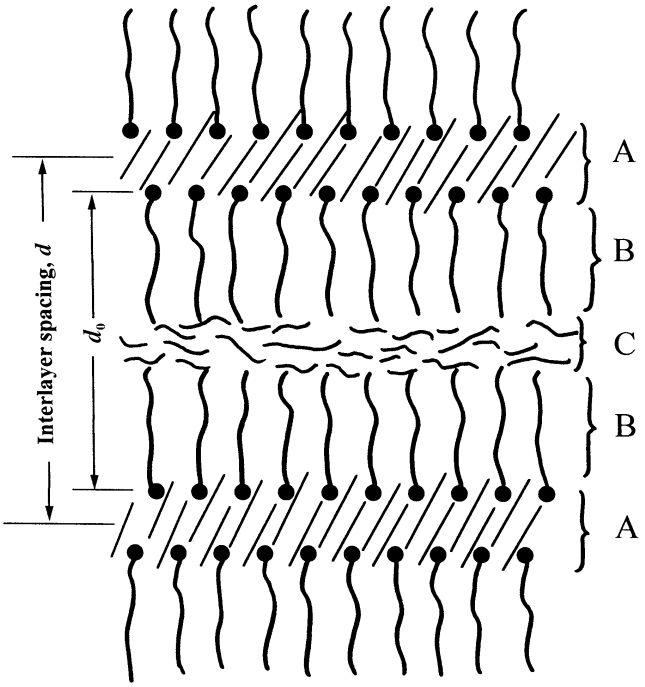

FIG. 12. The lamellar liquid crystal is described by three zones: A, water layer plus polar groups; B, hydrocarbon chain methylene group; C, hydrocarbon chain terminal methyl group and space between them.

TABLE 2
The Maximal Absorbance Wavelength and Molar Absorbance Coefficient of ODP in Laureth 4-H_2O-ODP System[a]

Phase ODP solubilized	H_2O% (wt)	λ_{max} (nm)	$\varepsilon \times 10^{-4}$ ($dm^3\ mol^{-1}cm^{-1}$)	ε (average) $\times 10^{-4}$ ($dm^3\ mol^{-1}cm^{-1}$)
LLC	55	309	3.12	
	54	310	3.11	
	48	307	2.95	
	47	309	2.91	
	45	309	3.01	
	45	309	3.21	
	40	309	2.65	
	34	310	2.91	2.98 ± 0.12
L_2	10	309	2.92	
	6	309	3.35	
	6	309	2.82	
	5	309	2.69	
	2	309	2.75	2.91 ± 0.25

[a]The statistic experimental error was calculated based on 90% confidence limits for the average value. Laureth 4: polyoxyethylene-4-laurylether. See Table 1 for other abbreviations.

TABLE 3
Values of Interlayer Spacing, d_0, and Solvent Penetration, α, in Lamellar Liquid Crystal Region[a]

Oil	Oil/Steareth 10 (w/w)	d_0 (Å)	α_w	$\alpha_{0,0}$
	0:100	61.6	0.52	0.67
Olive	10:90	63.5	0.47	0.84
	20:80	64.1	0.46	1.02
	0:100	61.6	0.52	—
ODP	10:90	62.0	0.43	0.99
	20:80	61.7	0.32	0.99

[a]See Table 1 for abbreviations.

in which d is interlayer spacing, d_0 is its value extrapolated to zero additive, α is a fraction penetration of a polar solvent from site A to site B (Fig. 12), and R is the volume ratio of added solvent to other components.

Limiting the α value to small values of R, Equation 1 is written:

$$d = d_0(1 + R)(1 - \alpha R) \quad [2]$$

and neglecting the square term in R:

$$d = d_0[1 + (1 - \alpha)R] \quad [3]$$

Algebraic manipulations give a simple expression for α:

$$\alpha = 1 - (\partial d/\partial R)/d_0 \quad [4]$$

With this background, the geometrical characteristics of the entire system may be obtained.

The values of α and d_0 for the LLC region of Steareth 10 are shown in Table 3. The difference between the influence by olive oil and by ODP is obvious from results in Figures 7 and 8 and Table 3. Addition of ODP has no effect on the d_0 value, the thickness of the lipid layer, B + C (Fig. 12), while addition of olive oil causes an increase of the d_0 value. The interpretation is straightforward; ODP is located in layer B of the LLC, while olive oil is at least partially localized in the C layer, the space between the terminal group of the surfactant (Fig. 12). A similar result was also obtained the Laureth 4 system (Table 4) with ODP.

The results may at first not be expected considering the molecular structure of ODP (Scheme 1). The extremely weak polarity of the ester group, combined with the branched hydrocarbon, would rather indicate a location in layer C (Fig. 12). However, the interaction between the ester group and the polar part of the surfactant favoring a location in layer B is significantly assisted by the influence of the benzene ring in ODP. As a matter of fact, as demonstrated early by Christenson *et al.* (23) and Friberg *et al.* (24), benzene has a preference for the polar parts in a colloidal association structure. It is so strong that the partition of benzene between the polar and nonpolar parts in a nonionic surfactant of the polyethyleneglycolalkylether type is 3:1 (25). Hence, it may safely be assumed that the benzene ring of ODP contributes to its preference for location in the B layer of the LLC of this investigation.

TABLE 4
Penetration, α, Interlayer Spacing, d_0, Values in LLC Region[a]

ODP/Laureth 4 (w/w)	d_0 (Å)	α (H_2O)
0:100	37.7	0.12
5:95	37.6	0.11
10:90	37.5	0.06
15:85	37.7	0.06

[a]See Tables 1 and 2 for abbreviations.

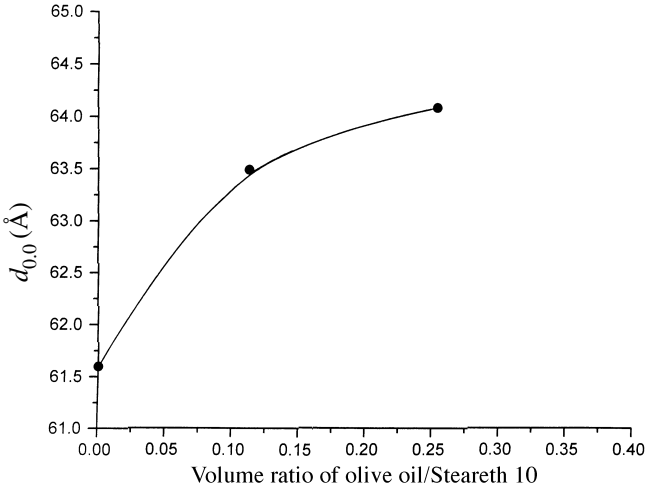

FIG. 13. Interlayer spacing without water, from Figure 2, $d_{0.0}$ with volume ratio of olive oil/Steareth 10. For abbreviations see Figure 1.

The x-ray data of the liquid crystal with added olive oil show results different from those with ODP. The increase of the thickness of the lipid layer, d_0 (Table 3), with an increased amount of olive oil (Fig. 8) reveals the oil to be partially located in position C (Fig. 12).

The partitioning of oil molecules between zones B and C may be estimated from the x-ray data, the d_0 values in Table 3. These d_0 values are given in Figure 13 as function of volume ratio of olive oil to Steareth 10. The points d_0 do not follow a straight line nor Equation 1, and curve fitting was used to obtain the necessary values.

The values fit a function

$$d_0{}^R = 61.6 + 21.1R - 49.2R^2 + 21.0R^3 \quad [5]$$

and the value of α for each R is calculated from the tangent to the curve in Figure 13 derived from Equation 2 with added indexing:

$$(d_0)_0{}^R = d_0{}^R - R{\cdot}\alpha d_0{}^R/\partial R \quad [6]$$

The values of the fraction of added olive oil penetrating into layer B (Fig. 12), $\alpha_{0,0}$, increased with the amount of oil and reached 1.02 for the highest amount of oil accepted by the LLC ($\alpha_{0,0}$, Table 3). A reasonable conclusion is that, when the added oil is no longer partitioned between layers C and B (Fig. 12) but becomes localized in layer B, the LLC becomes unstable. It is true that the values in Table 3 depend on the choice

FIG. 14. Microphotographs of phase changes during evaporation starting composition at A in Figure 6; the photographs correspond to A, B, C in Figure 6.

of function in Equation 5, but all tried polynomials resulted in $\alpha_{0,0}$ close to 1.0 for the highest amount of olive oil accepted into the LLC. The presence of olive oil at that level gives a structure in equilibrium with pure oil. The fact that the LLC is in equilibrium with pure oil without being influenced by the amount of water in the former is in support of the hypothesis that the saturation of layer C (Fig. 12) with oil leads to instability.

The conclusion about the location of ODP in the LLC is supported by the UV absorption spectra in Figures 10 and 11 with comparison in polar and nonpolar solvents. Using the LLC as a solubilizing medium, ODP showed an absorption region closer to that of polyethylene glycol than to that of decane. This is in accordance with the view that the sunscreen's UV-absorbing chromophores reside for the most part in amphiphilic layer B, which approaches the polar polyethylene oxide groups. It should also be noted that the absorption coefficient in LLC is as high as in other liquid medium. Note that the smaller polar component of Laureth 4, compared to Steareth 10, resulted in UV absorption, indicating a less polar environment in the LLC of the former.

Additional support for the conclusion about the location of ODP is provided by the values for the penetration fraction of water (Tables 2 and 3). Increasing the concentration of ODP leads to a reduction of the water penetration, a result that would be difficult to relate to a location of ODP in layer C (Fig. 12).

The phase diagrams provide an opportunity to evaluate the changes in the structure during evaporation of a formulation after its application, and a brief note on these conditions may be of value. Figure 6 shows two samples, A and D, with the projected evaporation paths as dashed lines. As seen in Figure 6 sample A consists of the LLC dispersed in water (Fig. 14A). The sample was not photographed between crossed polarizers because of difficulties with extremely long exposure times and movement of the droplets. However, visual observation revealed without doubt that the emulsion consists of droplets of liquid crystals, LLC (Fig. 6) in water. The phase diagram (Fig. 6) predicts the change of the emulsion to one layer of LLC (Point B in Fig. 6), after evaporation to one-half of the original weight, and this was confirmed experimentally (Fig. 14B). The phase diagram also predicts a change to an isotropic liquid after continued evaporation, (Point C in Fig. 6), also confirmed by the evaporation experiments (Fig. 14C). The final film was too thin to form a continuous cover, and the isotropic solution is found in patches (Fig. 14C).

Sample D (Figs. 6 and 15) should be an emulsion of ODP solution ODP/surfactant/water, by % (70:28:2%) droplets to a weight fraction of 0.13 in water (weight fraction 0.84), stabilized by a small amount (weight fraction 0.03) of the liquid crystal (25). The liquid crystal adheres to the droplets and is not observed in photo D of Figure 15. Evaporation of water changes the O/W emulsion to a lamellar liquid (LLC)-in-oil emulsion (Fig. 6, Point E), with the composition of the oil phase identical to the original one. At Point E, the weight fraction of liquid crystal is 0.16, and it may now be observed as distinct clusters (Fig. 15E). Even in this case, the liquid crystal should disappear with continued evaporation (Fig. 6). This was confirmed by the experimental results (Fig. 15).

Hence, the phase diagrams provide a means to predict the structural changes during evaporation of an emulsion that contains sunscreen molecules and, which is more important, to give a reliable prognosis of the final state of the formulation.

ACKNOWLEDGMENTS

This research was financed in part by ICI Surfactants (Wilmington, DE) and by the New York State Commission of Science and Technology at the Center for Advanced Materials Processing at Clarkson University, New York.

FIG. 15. Microphotographs of phase changes during evaporation starting composition at D in Figure 6, the photographs correspond to D,E,F phase in Figure 6.

REFERENCES

1. Patini, G., Perfluoropolyethers in Sunscreens, *Drug Cosmet. Ind. 143*:42–52 (1988).
2. Lowe, N.J., and N.A. Shaath, (eds.), *Sunscreens, Development, Evaluation, and Regulatory Aspects*, Marcel Dekker, New York, 1990.
3. Shaath, N.A., *Cosmetics Toiletries 101:*55–62 (1987).
4. Agrapidis-Paloympis, L.E., R.A. Nash, and N.A. Shaath, The Effect of Solvents on the Ultraviolet Absorbance of Sunscreens, *J. Soc. Cosmet. Chem. 38*:209–221 (1987).
5. Shaath, N.A., On the Theory of Ultraviolet Absorption by Sunscreen Chemicals, *Ibid. 38*:193–207 (1987).
6. Langlois, B., and S.E. Friberg, Evaporation from a Complex Emulsion System, *J. Cosmet. Chem. 44*:23–34 (1993).
7. Kleive, K., Formulating Sunscreen Products, in *Sunscreens, Development, Evaluation and Regulatory Aspects*, edited by N.J. Lowe, and N.A. Shaath, Marcel Dekker, New York 1990, pp. 235–266.
8. Elias, P.M., Lipids and the Epidermal Permeability Barrier, *Arch. Dermatol. Res. 270*:95–117 (1981).
9. Flynn, G.L., Mechanism of Percutaneous Absorption from Physicochemical Evidence, in *Percutaneous Absorption*, edited by R.L. Bronaugh and H.Z. Maibach, Marcel Dekker, New York, 1985, p. 17–42.
10. Landmann, L., The Epidermal Permeability Barrier, *Anat. Embryol. 178*:1–13 (1988).
11. Anderson, B.D., and P.V. Raykav, Solute Structure Permeability Relationships in Human Stratum Corneum, *J. Invest. Dermatol., 43*:280–286 (1989).
12. Dromgoole, S.H., and Maibach, H.I., Contact Sensitization and Photocontact Sensitization of Sunscreening Agents, in *Percutaneous Absorption*, edited by R.L. Bronaugh and H.Z. Maibach, Marcel Dekker, New York, 1985, pp. 313–340.
13. Matsui, T., and K. Tezuka, Cleansing Cosmetics Containing Nonionic Surfactants, Water and Oils, Japanese Patent 03,161,428[91,101,428] (1991).
14. Otsuka, N., and I. Tokimitsu, Cosmetic Moisturizing Compositions Fats and Oils, European Patent Applied EP 474,023 (1992).
15. Noda, A., K. Otsubo, and Harusawa, F., Hair Cleaning Compositions Containing Surfactants, Siloxanes and Hydrocarbon Oils, Japanese Patent 03,287,519[91,287,519] (1991).
16. Lin, S.Y., and W.H. Wu, Physical Parameters and Release Behaviors of W/O/W Multiple Emulsions Containing Cosurfactants and Different Specific Gravity of Oils, *Pharm. Acta. Helv. 66*:342–347 (1991).
17. Kiosseoglou, W., and G. Mourlidis, The Influence of Minor Surface Active Components of Olive Oil on Emulsification with Bovine Serum Albumin, *Colloids Surf. 59*:37–45 (1991).
18. Hodutu, M., Skin Moisturizer for Treatment of Eczema, Canadian Patent Applied CA 2,061,870 (1993).
19. Fuisz, R.C., Rapidly Dispersable Compositions Containing Polydextrose, European Patent Applied EP 570,327 (1993).
20. Jones, P.J.H., A.H. Lichtenstein, E.J. Schaefer, and G.L. Namchuk, Effect of Dietary Fat Selection on Plasma Cholesterol Synthesis in Older, Moderately Hypercholesterolemic Humans, *Arterioscler. Thromb. 14*:542–548 (1994).
21. Jickells, S., P. Gancedo, C. Nerin, L. Castle, and J. Gilbert, Migration of Styrene Monomer from Thermoset Polyester Cookware into Foods During High Temperature Application, *Food Addit. Contam. 10*:567–573 (1993).
22. Christenson, H., and S.E. Friberg, Spectroscopic Investigation of the Mutual Interactions Between Nonionic Surfactant, Hydrocarbon and Water, *J. Colloid Interface Sci. 75*:276–285 (1980).
23. Christenson, H., S.E. Friberg, and D.W. Larsen, NMR Investigations of Aggregation of Nonionic Surfactants in a Hydrocarbon Medium, *J. Phys. Chem. 84*:3633–3638 (1980).
24. Friberg, S.E., H. Christenson, G. Bertrand, and D.W. Larsen, Hydrocarbon Aromaticity and W/O Microemulsions Stabilized by Nonionic Surfactants, *Rev. Micelles 5*:105–111 (1984).
25. Friberg, S.E., P.O. Jansson, and E. Cerderberg, Surfactant Association Structure and Emulsion Stability, *J. Colloid Interface Sci. 55*:614–623 (1976).

[Received August 23, 1996; accepted March 20, 1997]